ELSEVIER

Journal of Power Sources 70 (1998) 258–268

JOURNAL OF POWER SOURCES

Modeling electrochemical performance in large scale proton exchange membrane fuel cell stacks

J.H. Lee [a,*], T.R. Lalk [b], A.J. Appleby [c]

[a] *Los Alamos National Laboratory, Los Alamos, NM 87545, USA*

[b] *Dept. of Mech. Eng., Texas A&M University, College Station, TX 77843-3123, USA*

[c] *Center for Electrochemical Studies and Hydrogen Research, Texas Engineering Experimentation Station, Texas A&M University, College Station, TX 77843-3402, USA*

Received 14 April 1997; accepted 11 June 1997

Abstract

The processes, losses, and electrical characteristics of a Membrane-Electrode Assembly (MEA) of a Proton Exchange Membrane Fuel Cell (PEMFC) are described. In addition, a technique for numerically modeling the electrochemical performance of a MEA, developed specifically to be implemented as part of a numerical model of a complete fuel cell stack, is presented. The technique of calculating electrochemical performance was demonstrated by modeling the MEA of a 350 cm^2, 125 cell PEMFC and combining it with a dynamic fuel cell stack model developed by the authors. Results from the demonstration that pertain to the MEA sub-model are given and described. These include plots of the temperature, pressure, humidity, and oxygen partial pressure distributions for the middle MEA of the modeled stack as well as the corresponding current produced by that MEA. The demonstration showed that models developed using this technique produce results that are reasonable when compared to established performance expectations and experimental results. © 1998 Elsevier Science S.A.

Keywords: Fuel cells; Electrochemistry; Reaction mechanisms; Mathematical modeling; Design

1. Introduction

A fuel cell is an electrochemical device that combines hydrogen and oxygen, with the aid of electrocatalysts, to produce electricity. As shown in Fig. 1, a fuel cell consists of a negatively charged anode, a positively charged cathode, and an electrolyte which transports protons from the anode to the cathode but blocks electrons, forcing them to move through the external load. A state of the art, low temperature fuel cell has an electrical potential of about 0.7 V when generating a current density of approximately 300–500 mA/cm^2. Practical fuel cell power systems will require a combination of several cells in series (a stack) to satisfy the voltage requirements of specific applications. Potential applications for fuel cells include remote power generation, vehicle power plants, and large multi-megawatt power generating stations.

To date, most research involving Proton Exchange Membrane Fuel Cells (PEMFC), named for the type of electrolyte used, has emphasized improving the electrochemical performance of laboratory scale single cells. Only limited research efforts have been directed at investigating fuel cell stacks and complete systems. Components of a complete system include fuel and oxidant (air) supply, fuel cell stack, water and thermal management, current collection, and control systems. A schematic diagram of a complete fuel cell power system is given in Fig. 2.

In order for these systems to become efficient and affordable sources of electrical power a greater understanding of complete fuel cell systems, and the parameters that affect them, is needed. Fuel cell systems are influenced by many parameters that affect performance, and each of these parameters can have a range of possible values. Investigating each parameter independently and/or all possible combinations of parameters using laboratory experiments would be costly and time consuming.

A method for investigating the effects of parameters and combinations of parameters that would reduce the

* Corresponding author.

PII S0378-7753(97)02683-9

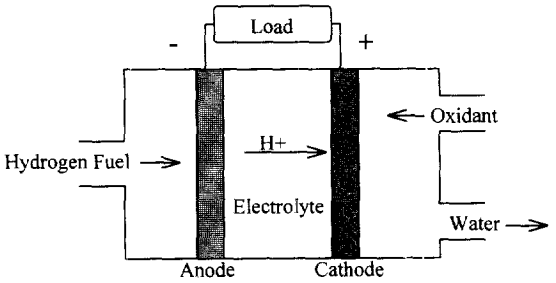

Fig. 1. Schematic diagram of a fuel cell.

amount of time and money required is numerical modeling. A numerical model that calculates all the physical properties of a fuel cell stack is a valuable research tool for investigating system parameters. This is because of the ease with which models can be modified to simulate various configurations and operating conditions. For example, to investigate the relationship between the active area of the MEA and system performance several laboratory test fixtures would be needed where as the same investigation could be conducted using a numerical model by changing a few lines of computer code.

Although a numerical model is useful for investigating stack parameters the effort required to develop a model can be considerable. For example, the individual fuel cell, or Membrane-Electrode Assembly (MEA), is a component of a fuel cell stack that requires considerable effort to model. This is due to the complexity of the physical processes that occur in the MEA during stack operation including diffusion, capillary action, and electron and ion transfer. These will be discussed in detail below.

Several one dimensional models of single fuel cells exist, however their main focus is to investigate electrochemical processes of single fuel cells [1–3]. These models model the physical processes using equations derived from basic principles and experimentally determined constants. The calculations required for these models is too extensive to be used in a comprehensive model of a complete stack.

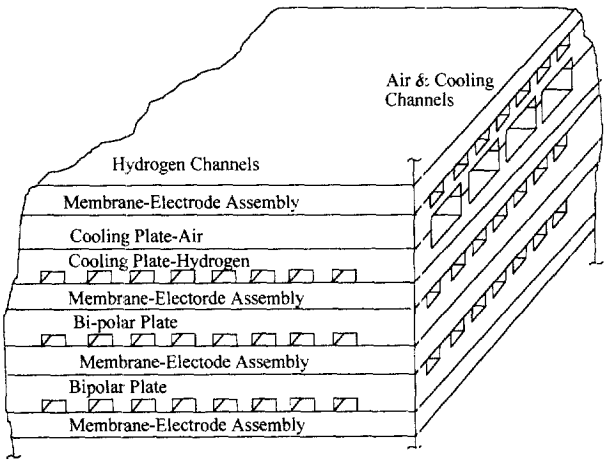

Fig. 2. Schematic diagram of a fuel cell stack.

A need exists for a technique for determining MEA electrochemical performance that does not require a large number of calculations. In addition, the technique needs to be able to be integrated into a numerical model of a complete fuel cell stack so that complete fuel cell power systems may be modeled. Consequently the objective of this investigation was to develop such a technique.

The theory used to develop the modeling technique includes the electrical and electrochemical characteristics of the membrane and electrodes of the fuel cell and fuel cell stack. Electrical characteristics used when developing the model include the equal potential nature of the electrodes and the series arrangement of the cells in a stack. In order to simplify the calculation of the electrochemical characteristics of the MEA an empirical equation that represents the relationship between the current and voltage produced by a MEA was used. These characteristics were combined to develop a modeling technique that calculates MEA performance without requiring a large number of calculations.

The remainder of this paper describes the processes, losses, and electrical characteristics of a MEA, as well as introduces a modeling technique that accounts for these phenomenon without requiring extensive calculations. Implementation of the modeling technique is described and demonstrated by modeling the MEA of a 350 cm^2 PEMFC in combination with a numerical model of the remaining components of a 125 cell stack. This composite model is used to simulate operation of the stack for typical vehicle operating conditions. Sample output from this simulation is presented. Finally, the process is summarized and observations concerning its usefulness made.

2. Theory

The electrochemical and electrical characteristics of a MEA are difficult to represent with a numerical model due to their complexity. A model must account for the delivery and removal of the gases, the kinetics of the electrochemical reaction, and the electrical properties of the materials used to construct the MEA. Section 2.1 discusses the physical processes, polarization, and electrical characteristics of a MEA that should be accounted for in a numerical model of a MEA. The following discussion pertains primarily to PEMFC membrane-electrode assemblies, a diagram of which is given in Fig. 3.

2.1. Physical processes

There are several physical processes that must occur in a MEA in order for the electrochemical process to work. These processes include gas diffusion, electrochemical reactions, and ion and electron transfer. Section 2.1 will discuss each of these process.

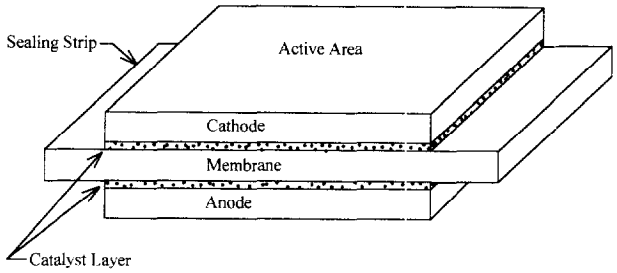

Fig. 3. Schematic diagram of a membrane-electrode assembly of a proton exchange membrane fuel cell.

2.1.1. Gas diffusion

Gas diffusion is the mode of transport for the gases in both the anode and the cathode. The fuel diffuses through the anode and oxidant through the cathode. At the anode hydrogen, or a hydrogen rich mixture if a reformed fuel is used, diffuses into the electrode and impurities diffuse out. Oxygen, or oxygen and nitrogen if air is used, diffuse into the cathode and water and impurities diffuse out. If the process gases are humidified water also diffuses inward through the electrodes.

The gases move from the flow channels of the bipolar plate through the porous electrodes to the reaction sites near the membrane. The gases move from an area of greater concentration, the flow channel of the bipolar plate, to an area of lesser concentration, the electrode-membrane junction. They pass into the electrode at a rate proportional to the concentration gradient.

The most common method for modeling this process is to use the Stefan–Maxwell equation [1]. That is,

$$\frac{\mathrm{d}x_i}{\mathrm{d}z} = RT\sum_j \frac{x_i N_j - x_j N_i}{PD_{ij}} \tag{1}$$

Where x is the mole fraction of constituent i, z is perpendicular distance through the electrode, R is the universal gas constant, T the gas temperature, N is the molar flux, P is the pressure, and D is the diffusion coefficient. This equation relates the rate of species transfer to the concentration gradient. For a MEA, the diffusion constant is a function of the density, temperature, and pressure of the gases being diffused and the electrode materials. The value of these diffusion constants is determined experimentally.

2.1.2. Capillary action

As the gases approach the reaction sites (catalyst locations) they begin to flow via capillary action. The application of the catalyst and other materials to the activation layer of the electrodes reduces the size of the passages the gases move through. This reduces the amount of gas that flows by way of diffusion. The remainder of the gas that is needed for the reactions moves via capillary action.

Capillary action results from the affinity flow channel materials have for the fluid flowing through the channels. This is the same force that causes a meniscus in columns of fluid. As the channels reduce in size the force that results from the wall affinity becomes large enough to pull the fluid through the channel [4].

As the electrochemical reactions proceed the process gases are consumed and replacement gas diffuses to the reaction sites as a result of the concentration gradient via capillary action. The capillary action near the reaction sites aids the performance of the electrodes by dispersing the gas, increasing the probability it will reach a reaction site. The effect the capillary action is incorporated into the experimentally determined diffusion coefficient and is therefore neglected when modeling the MEA.

2.1.3. Electrochemical reactions

There are two electrochemical half-cell reactions that occur in a MEA, one at the anode and one at the cathode. The break down of hydrogen into hydrogen ions and electrons occurs at the anode. The stoichiometric chemical equation that represents the anode half reaction is given by Eq. (2).

$$H_2 \Leftrightarrow 2H^+ + 2e^- \tag{2}$$

In a numerical model Eq. (2) is used to calculate the amount of hydrogen that is needed for the process to occur.

The half-cell reaction at the cathode combines oxygen, hydrogen ions, and electrons to form water. The Stoichiometric chemical equation that represents the cathode half-cell reaction is given by Eq. (3).

$$4H^+ + O_2 + 4e^- \Leftrightarrow 2H_2O \tag{3}$$

The amount of oxygen required and the amount of water produced by the process are calculated using Eq. (3) in combination with Eq. (2).

2.1.4. Ion transfer

The ions produced at the anode must be transported across the membrane to the reaction sites in the cathode [5]. The transport process involves the interaction of the ions with each other as well as with water molecules in the membrane. The acid chains that make up the membrane do not contribute directly to the transport process. Their function is to maintain the structural integrity of the membrane and be electronic insulators.

The initial force that moves the ions is the positive potential at the anode-membrane interface. This potential results from the build up of hydrogen ions at the interface. This force repels the positively charged ions, pushing the outer ions away from the anode.

Water molecules in the membrane provide the medium for the ions to move. The slight negative charge of the hydrogen side of the water molecule attracts the positive hydrogen ion and if an ion come in contact with a water molecule it may become attached to it. Since the attraction

is weak the ion is easily separated from the water molecule and it may move to the next water molecule it comes in contact with. The probability of these occurrences depends on many things including the number of ions to be transported, the amount of water in the membrane, the thickness of the membrane, etc. A net drift of ions occurs in the direction of the negative potential; for the ions the cathode side of the membrane is the negative potential.

An example of how this process has been modeled is given by Springer and Zawodzinski [1]. The membrane portion of Springer's model consists of several empirical equations that calculate the water content of the membrane, the net movement of water toward each electrode, and the resistance and voltage drop across the membrane. The model uses 12 equations and an iterative solution to calculate the performance of the membrane.

2.1.5. Electron transfer

The electrons released by the electrochemical reaction must travel from the anode to the cathode without moving through the membrane as this would result in a short circuit. Specifically, the electrons travel from a reaction site in the anode, through the gas diffusion region of the anode, across the bipolar plate, through the diffusion region of the adjoining cathode, and finally to a reaction site in the cathode. The electrons choose this path because they prefer to move through materials that consist of molecules with loosely held electrons.

The process of moving electrons through a material consists of electrons colliding with molecules of the material and transferring their energy to the molecule. The excited molecules then release an electron which collide with another molecules. A net drift of electrons occurs in the direction of the positive potential; for the electrons the positive potential is the cathode.

The electrons do not travel through the membrane because the perfluoropolymer backbone and acid groups that make up the membrane are electric insulators. This is one property that determines desirable membrane material. Others desirable properties include structural stability, low porosity, and low resistance to the movement of ions.

2.2. Process polarization

Losses associated with a MEA are separated into activation, ohmic and concentration polarization. Each polarization is influenced by many factors including the type of electrocatalyst used in the cathode and anode, and the manner in which it is applied, the fuel and oxidant used to operate the fuel cell, the materials used in construction, and the manner in which the fuel cell is operated. Section 2.2 discusses the maximum theoretical MEA voltage and each type of polarization including factors that affect each polarization and ways to reduce the losses.

2.2.1. Theoretical voltage

The maximum theoretical voltage a MEA can produce is a function of the fuel used [6]. The theoretical voltage (E_T) is a function of the change in free energy of the fuel (ΔG), the number of electrons involved in the overall process n, (4 for the hydrogen/oxygen reaction), and Faraday's constant F, (96,487 C/mole).

$$E_T = \Delta G/nF \quad (4)$$

Since the free energy of the fuel is a function of temperature the theoretical voltage is also affected by temperature. For most reactions the theoretical voltage increases with increasing temperature.

2.2.2. Activation polarization

Activation polarization is a result of the need to effect electron transfer and to break and form chemical bonds in the anode and cathode [7]. At the anode, hydrogen (fuel) molecules comes in contact with the catalyst surfaces and are adsorbed. This process entails breaking the bond in the fuel molecule and forming a new bond between the resulting atom and the catalyst surface. This is followed by electron transfer and desorption of protons, following well-known reaction mechanisms [8].

A similar process occurs at the cathode except the oxygen atom is adsorbed on the catalyst surface and hydrogen ions and electrons are then discharged. After an overall transfer of four electrons and four protons in successive steps, with breaking of the O–O bond two water molecules are formed.

Irreversible energy is required to break and reform all of the bonds that change during the electrochemical reaction. This energy is supplied by the fuel used in the fuel cell. As a result, the amount of energy that is available to produce electric power is reduced.

The amount of the reduction is a function of the rate of the reaction. This is because an increase in reaction rate requires an increase in the process gas flowrate and a corresponding increase in the process gas kinetic energy. The increased kinetic energy aids in breaking the bonds thereby reducing the energy that must be supplied by the fuel for that purpose. Additional means of reducing activation polarization include increasing the active area of the electrode, increasing the utilization of a suitable catalyst, and increasing operating temperature.

2.2.3. Ohmic polarization

Ohmic polarization is caused by electrical resistance losses in the cell. Electrical resistance is found in the electrodes, the membrane (ionic), the fixtures that connect the MEAs, and the interfaces between each component. Ohmic polarization can be reduced by using components that have a high electrical conductivity and reducing the thickness of the membrane.

2.2.4. Concentration polarization

Concentration polarization is the result of resistance to mass transport of gases to the reaction sites. This includes

transporting process gases to, and removing product water and impurities from, the reaction sites. Lower than ideal quantities of process gases at the reaction sites decreases the number of chemical reactions at the electrodes resulting in a loss in MEA voltage. Similarly, a build up of product water and impurities dilute the process gases, reducing the effectiveness of the reaction sites. Concentration polarization can be reduced by increasing the operating pressure, using high surface area electrodes, and reducing the thickness of the electrodes so there is a shorter path for the gases to diffuse through.

A combination of these three types of polarization results in a voltage–current relationship for a MEA where the voltage decreases as increasing current. Each type of polarization is dominant in a particular current region. Fig. 4 shows a typical voltage–current (polarization plot) for a Proton Exchange Membrane Fuel Cell MEA.

The difference between the theoretical and open circuit voltage (zero current) is a result of activation polarization at the oxygen electrode. Further, activation polarization causes the reduction in voltage in the low-current regions of MEA operation. The steep slope of the initial portion of the curve is an indication of the activation polarization. As the current increases, the slope of the curve becomes less steep. This is a result of the activation polarization becoming less significant due to the increase in other polarization phenomena, notably concentration and ohmic effects.

The ohmic polarization becomes significant in the intermediate current range as indicated by the linear nature of the middle region of Fig. 4. This is consistent with the linear nature of ohmic resistance. The inflection point between the initial and middle sections of the polarization curve clearly indicates the demarcation between the activation and ohmic regions of fuel cell operation. The inflection point also indicates the increased influence of ohmic polarization with increasing current.

A second inflection point and the steep decline in voltage in the highest current region of Fig. 4 result from concentration polarization. At the highest current range process gases are needed faster than they can move to the reaction sites. The result is a depletion of ions and electrons at the electrode-membrane interfaces and a corresponding reduction in cell potential. The steep decline in the polarization curve is consistent with the relationship between concentration gradient and diffusion rates.

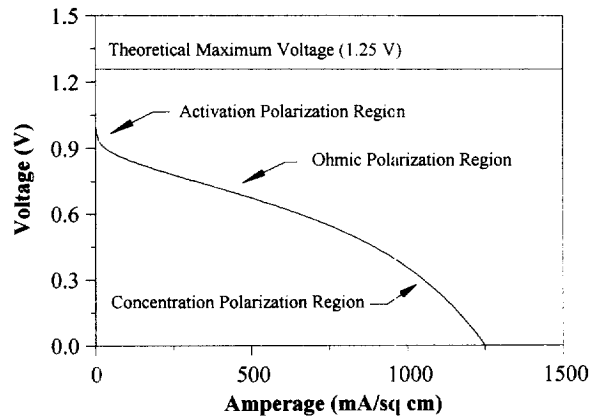

Fig. 4. Typical polarization curve for a proton exchange membrane fuel cell.

2.3. Electrical characteristics

Fuel cell MEAs have electrical characteristics that need to be accounted for in a numerical modeling technique. These include the voltage and current of a MEA. Each characteristic is described in Section 2.3.

2.3.1. Voltage characteristic

The voltage characteristic of a MEA is such that all positions on the MEA have the same voltage drop. The surfaces of a MEA are equipotential surfaces such that the voltage drop across the membrane is not dependent on position. Different MEAs in the same stack can have different potentials, but every MEA has only one potential regardless of its surface area. This characteristic is a result of using low ohmic resistance materials in the construction of the electrodes.

2.3.2. Current characteristic

The other electrical characteristic that must be accounted for in modeling is that each MEA in a stack must produce the same total current. Fuel cell stacks are composed of multiple MEAs arranged in electrical series to increase the voltage of the overall stack. A result of being arranged in electrical series is that the electrons freed by the reduction of hydrogen at the anode will be used by the cathode of the adjoining MEA to form water and complete the reaction. Therefore, each MEA in a fuel cell stack must produce the same number of electrons.

The high conductivity of the electrode materials enable the electrons to migrate through the electrodes in various directions until they find a suitable reaction site in the cathode. This migration ability allows the location of electron production to vary between MEAs. One MEA may produce a majority of its electrons in the center of the active area whereas another MEA may produce electrons equally throughout the active area. The only physical restriction is that each MEA produce the same total number of electrons.

The complexity of the above processes make a model of a MEA developed from basic principles impractical for use in a numerical model of a complete fuel cell stack. This is due to the large number of calculations required to determine the performance, and satisfy the electrical characteristics, of each MEA in the model. Therefore, a simplified technique for modeling MEA performance is needed in a numerical model of a complete fuel cell stack.

3. Application to large scale models

In order to model a complete fuel cell power system a simplified approach for estimating the performance of a MEA is needed that can account for the physical processes, process polarization, and electrical characteristics that exist in large scale stacks. A technique using empirical relationships to model the physical processes and process polarization of the MEAs, the electrical characteristics of the MEAs, and the stack load to calculate the electrical performance of a stack was developed. It was anticipated that models developed using the technique would be included in larger dynamic models of complete fuel cell power systems. The remainder of this section describes the modeling technique and how it is used to estimate the performance of a MEA.

The MEA modeling technique uses empirical equations, derived using data collected from laboratory scale single cells, to model the physical processes and process polarization of the MEAs. The empirical equation that is used for PEMFC stack models relates the voltage of a MEA (V_e) to its current (i_e) [9]. That is,

$$\begin{aligned} V_e(T,p,p_{O_2},\phi) &= V_o(T,p,p_{O_2},\phi)_e - b(T,p,p_{O_2},\phi)\log(i_e) \\ &\quad - R(T,p,p_{O_2},\phi)i_e - m(T,p,p_{O_2},\phi) \\ &\quad \times \exp\left[n(T,p,p_{O_2},\phi)i_e\right] \\ &\quad - b(T,p,p_{O_2},\phi)\log\left(\frac{p}{p_{O_2}}\right) \end{aligned} \quad (5)$$

Where V_o is the open circuit voltage, T is the absolute temperature, p_{O_2} is the partial pressure of oxygen, p is the total pressure, and f is the relative humidity of the process air. The remaining terms b, R, m, and n are all empirical equation constants. This equation represents the polarization curve shown in Fig. 4.

Each of the terms in Eq. (5) represent the losses described in Section 2. The open circuit voltage (V_{oc}) and the logarithm associated with the current (i_e) account for the activation polarization. These two terms are a form of the Tafel Equation; an empirical equation that is used to describe the voltage drop due to activation polarization [8].

The product of R and the current account for the ohmic polarization. The expression is Ohms Law of electrical resistance. The constant R accounts for the ohmic resistance of the membrane and both electrodes, the charge-transfer resistance of the half-cell reactions, and the ohmic resistance of the test fixture.

The exponential term and the pressure ratio logarithm account for the concentration polarization. The exponential term is an empirical expression developed by comparing Eq. (5), without the exponential term, to experimental data. The pressure ratio logarithm is a form of the Nerst Equation, an equation used primarily to describe potential changes in the cathode. Both logarithmic terms are multiplied by the constant b even though they account for different polarization. This is because the numerical values of the constants were the same [6,9].

The values of the constants in Eq. (5) vary depending on the type of MEA, the oxidant used, and the local temperature, pressure, humidity, and oxygen concentration at the reaction sites. It is anticipated that there are variations of the temperature, pressure, humidity, and oxygen concentration across individual MEAs in large scale fuel cell stacks. Therefore, the MEA model was developed as a two dimensional model (length and width of the MEA) so that variations in temperature, pressure, humidity and oxygen concentration that exist anywhere on the surface of the MEA can be included in the model.

To account for differences in the local temperature, pressure, humidity, and oxygen concentration that may occur across a MEA a grid work of computational elements or blocks is established as shown in Fig. 5. The temperature, pressure, humidity, and oxygen concentration of an element is assumed to be uniform. Each element is assumed to interact with the blocks that surround it and the bipolar plates it comes in contact with (see Fig. 2). The size and shape of the computational element depends on the variation expected. The larger the anticipated variation, the smaller the computational blocks.

The point on the polarization curve (Fig. 4) corresponding to the operation of each individual element of the MEA is in general determined by estimation the voltage and using Eq. (5) to calculate the corresponding current. The procedure for the initial time step requires a different procedure. The procedure for the initial case as well as the general case are explained below.

For the initial time step it is assumed that the stack starts with a uniform temperature, pressure, humidity, and partial pressure of oxygen (usually ambient). Thus initially, the same polarization curve represents the performance of every power producing computational element of every MEA in the stack and each MEA will have the same voltage. The total stack load requirement (extremely specified) is divided by the number of MEA computational

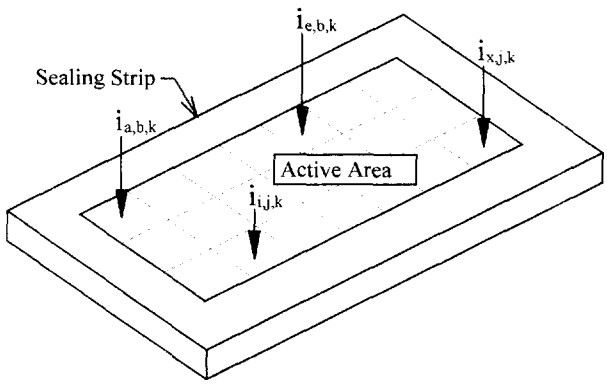

Fig. 5. Schematic diagram of a membrane-electrode assembly of a fuel cell stack divided into computational elements.

elements to determine the initial power requirement for each element, P_e.

$$P_{\text{Load}} = \sum_{k=1}^{K}\sum_{j=1}^{J}\sum_{i=1}^{I}(P_e)_{i,j,k} = \sum_{k=1}^{K}(P_{\text{MEA}}) = IJK(P_e)_{i,j,k} \quad (6)$$

$$(P_e)_{i,j,k} = \frac{P_{\text{Load}}}{IJK} \quad (7)$$

Where P_{Load} is specified by the external load applied to the stack and there are IJK total computational elements (IJ per MEA and K MEAs).

An empirical expression for elemental power, P_e, is determined by multiplying Eq. (5) by elemental current. That is,

$$\begin{aligned} P_e(T,p,p_{O_2},\phi) &= i_e V_o(T,p,p_{O_2},\phi)_e \\ &- b(T,p,p,_{O_2},\phi)i_e\log(i_e) - R(T,p,p_{O_2},\phi)i_e^2 \\ &- m(T,p,p_{O_2},\phi)i_e\exp\left[n(T,p,p_{O_2},\phi)i_e\right] \\ &- b(T,p,p_{O_2},\phi)i_e\log\left(\frac{p}{p_{O_2}}\right) \end{aligned} \quad (8)$$

With P_e specified Eq. (8) is solved iteratively for the corresponding element current i_e.

Since the equation is quadratic in i_e there will be two possible solutions. That is, the point at which the element will operate, supplying the required power, could be either of two current values. This is evident as two possible conditions on the typical power curve shown in Fig. 6. The lower of the two current values is selected because this is what would actually occur in a situation when the load is increased from zero current to the specified operating power.

The element current is then used in Eq. (5) to calculate the required element voltage which is equal to the MEA voltage.

$$(V_e)_{i,j,k} = V_{\text{EMA}} \quad (9)$$

After the initial time step a different procedure is used to determine the elemental operating conditions. An initial estimate of the MEA voltage is obtained by assuming a value equal to the previous time step voltage. That is,

$$(V_{\text{EMA}})_k^t = (V_{\text{EMA}})_k^{t-1} \quad (10)$$

The current through each element of each MEA $(i_e)_{i,j,k}$ is calculated iteratively using the MEA voltage, V_{MEA}, and Eq. (5). In general there will be a different Eq. (5) (polarization curve) that is applicable to each element of the MEA depending on the local values of temperature, pressure, humidity, and oxygen concentration. These local values of temperature, pressure, humidity, and oxygen concentration are calculated by other sub-routines of the fuel cell system model and are accounted for in the constants (V_o, b, R, m, n) of Eq. (5).

The summations of the calculated values for the elemental current and power produced by each MEA are then compared to the specified total load and current requirements. This is done to determine if there is agreement between the sum of the local values and the overall requirements. The total current produced by the kth MEA in the stack is calculated by summing the contributions to the total MEA current from all of the computational elements.

$$(i_{\text{MEA}})_k = \sum_{j=1}^{J}\sum_{i=1}^{I}(i_e)_{i,j,k} \quad (11)$$

In an actual fuel cell stack the current produced by each MEA is the same since they are in electrical series (see Fig. 2). Thus, it is a requirement that the calculated current produced by each MEA be the same.

The total power produced by a particular MEA is determined by multiplying the current for each element of the MEA by the voltage for that MEA and then summing the resulting elemental powers. That is the element power is represented by Eq. (12).

$$(P_e)_{i,j,k} = (i_e)_{i,j,k}(V_{\text{EMA}})_k \quad (12)$$

The power produced by a particular MEA is given by Eq. (13).

$$(P_{\text{MEA}})_k = \sum_{j=1}^{J}\sum_{i=1}^{I}(P_e)_{i,j,k} \quad (13)$$

Finally the total power produced by the entire stack is calculated with Eq. (14).

$$P_{\text{stack}} = \sum_{k=1}^{N}(P_{\text{EMA}})_k \quad (14)$$

Where N is the number of MEAs in the stack being modeled.

The calculated total power produced by the stack is then compared to the specified load requirement. The comparison routine checks to determine if the calculated power is within an acceptable range. That is, it determines if the power produced is not only greater than the load requirement, but also that it is not more than a prescribed percentage greater.

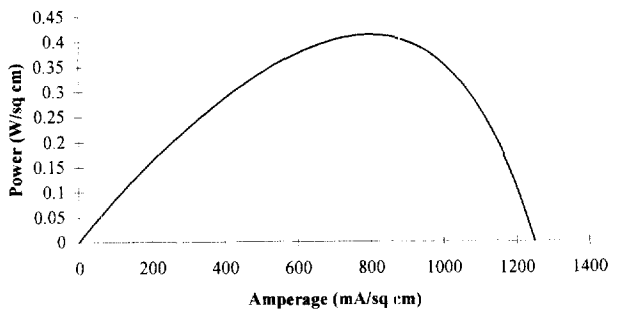

Fig. 6. Typical plot of the power produced by a MEA as a function of current produced.

The difference between the calculated power produced and the prescribed load is used to initiate adjustments to the voltage if the power produced is not in the acceptable range. This power deviation is determined by subtracting the externally specified load from the calculated power produced.

$$\Delta P_{\text{Stack}} = P_{\text{Stack}} - P_{\text{Load}} \quad (15)$$

Another check is made for compliance with the requirement that the current through all MEAs be the same. This is done by determining a current variation among MEAs, δi_{MEA}, which is the difference between the MEA current extremes. The current variation is given by Eq. (16).

$$\delta i_{\text{MEA}} = (i_{\text{MEA}})_{\max} - (i_{\text{MEA}})_{\min} \quad (16)$$

The current variation is compared to a prescribed acceptable difference. If the difference is within the acceptable limit, and the total stack power is within its acceptable range, the program will advance to the next time step. Otherwise, corrections are initiated.

Corrections to the power and current are made by calculating new values for the voltages of all the MEAs, recalculating the corresponding currents and powers, and comparing the new value for the stack power produced to the prescribed load and the current variation among the MEAs to the acceptable limit. Experimental observations of fuel cell stacks have indicated that variations in voltage drop across individual MEAs in a stack exist (Swan, private communication, 1996). As a result, the MEA model allows the voltage drop across individual MEAs to vary.

The new values for the voltages are calculated using an equation that accounts for the power and current of each individual MEA as well as the overall stack power and current.

$$(V_{\text{EMA}})_k = \frac{K(P_{\text{EMA}})_k}{(i_{\text{MEA}})_{\text{mean}} + (K-1)(i_{\text{EMA}})_k} + \frac{\Delta P_{\text{Stack}}}{K(i_{\text{EMA}})_k} \quad (17)$$

The $(i_{\text{MEA}})_{\text{mean}}$ term is the mean value for the MEA currents. The values for the variables in this equation are those from the most recent iteration. Thus the new value is always based on the previous one. The derivation of Eq. (17) is provided in the Appendix A.

The iteration process continues with all stack and MEA quantities updated until the current variation among MEAs and calculated stack power produced are within acceptable limits. The number of iterations required depends on the prescribed limits and the size of the fuel cell stack being modeled. The closer the prescribed limits and the larger the fuel cell stack the greater the number of iterations that will be required.

Once the current and voltage are calculated the values are transferred to the fuel cell power system model. The system model uses these values to calculate the performance parameters for the power system being modeled. This process is repeated for each time step modeled by the fuel cell power system model.

4. Results and discussion

Implementation of the modeling procedure is demonstrated by modeling the MEA of a 350 cm^2 PEMFC in combination with a numerical model of a 125 cell stack. The remainder of this section describes the MEA modeled, the design and operating parameters used in the model of the complete fuel cell power system, and the load conditions that were applied to the model. Sample output from the complete model pertaining to the MEA is shown and discussed, and observations concerning the modeling technique were made.

The MEA modeled consisted of a Nafion® 115 Proton Exchange Membrane and two carbon cloth electrodes both impregnated with 0.3 mg Pt/cm^2. The technique used to construct the membrane assembly was developed by the Center for Electrochemical Systems and Hydrogen Research (CESHR) at Texas A&M University. The active area of the MEA modeled was 350 cm^2, 25 cm long and 14 cm wide.

The model of the MEA was incorporated in a model of a PEM fuel cell power system model. The model consists of a 125 cell, 350 cm^2 fuel cell stack. The MEA was computationally divided into 350 computational elements, 1 cm^2 each, for calculating electrochemical performance. Table 1 lists the details of the stack design and the operating conditions. A complete description of the model-

Table 1
Design specifications for the fuel cell stack

Parameter	Description
Operating	
Pressure	5 atm
Temperature	50°C
Humidity	100% at stack entrance
Stoichiometry	Air = 2
	Hydrogen = 1.2
Design	
Membrane-electrode assembly	
Membrane	Nafion® 115
Catalyst	0.3 mg platinum/cm^2 for both electrodes
Electrode	CESHR
Stack	
Bipolar plate area	350 cm^2
Aspect ratio	2
Number of cells	125
Bipolar plate material	Coated corrugated aluminum
Flow configuration	Counter flow
Gas delivery strategy	Parallel flow/external manifolds
Cooling plate material	Coated corrugated aluminum
Cooling fluid	Air (cross flow)
Cooling plate frequency	1 cooling plate/2 cells
Stack construction	Bonding

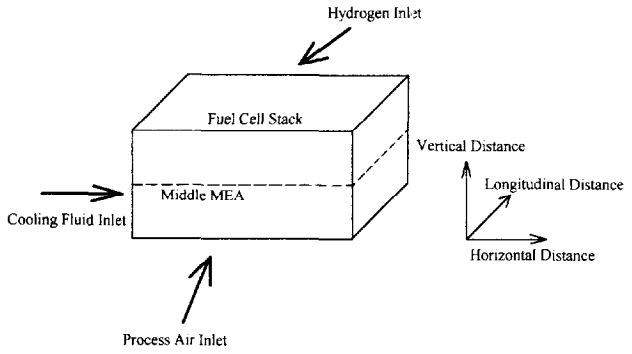

Fig. 7. Schematic diagram of a fuel cell stack describing the orientation of the plots of the simulation results (Figs. 8–12).

ing technique used to develop the model of the power system is given by Lee and Lalk [10].

The load used in the model was a sine wave that closely approximated the Generic Simplified Federal Urban Driving Schedule (GSFUDS) [11]. This cycle has been proposed for testing electric vehicles, a potential application for PEM fuel cell power systems. The load has units of kW and is given in Eq. (18).

$$P_{\text{Load}} = 8 + 2\sin\left(\frac{\text{time} \cdot \pi}{15}\right) \tag{18}$$

The fuel cell power system model was configured as described above and operated on a Silicon Graphics Power Challenge XL® Supercomputer. The following results were obtained using the power system model to simulate 15 min of operation. Upon completion of the simulated time the temperature, pressure, humidity, oxygen partial pressure, and current distributions of the MEA at the middle of the stack were recorded. Fig. 7 is a schematic diagram of a fuel cell stack to assist in orienting the plots of the results and Figs. 8–12 are the results from the simulation.

Fig. 8 is a plot of the temperature distribution for the middle MEA of the PEMFC system model. As anticipated the temperature of the MEA increases with increasing

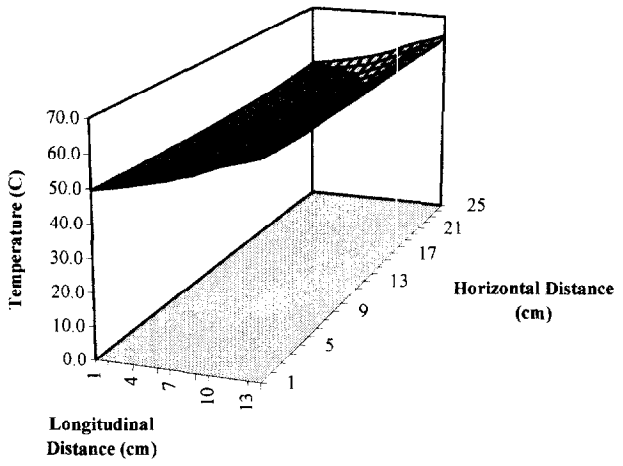

Fig. 8. Plot of the temperature distribution of the center MEA of a PEMFC stack after 15 min of simulation.

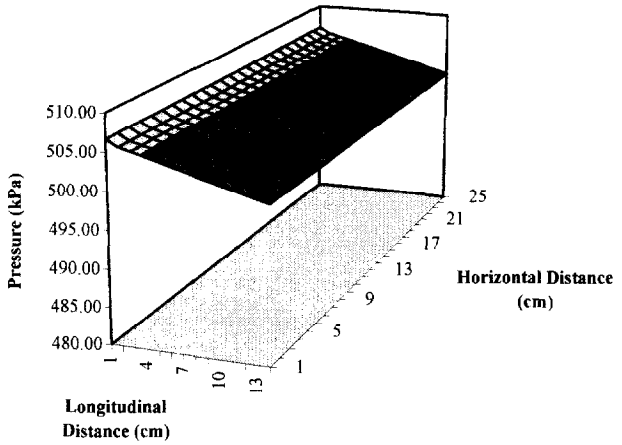

Fig. 9. Plot of the pressure distribution of the center MEA of a PEMFC stack after 15 min of simulation.

distance along the process air flow channels (longitudinal distance). The lower temperatures in the middle of the plate compared to the outer edges indicates that the cooling system has a significant affect on stack temperature. The outer edges are at a higher temperature because the sealing strip (see Fig. 5) is not cooled and acts as a thermal capacitor. At a given longitudinal distance the difference in temperature between the center of the MEA and the outer edges is less than 2°C and does not significantly affect performance. All temperatures in Fig. 8 are within the acceptable operating range for a PEMFC.

Fig. 9, a plot of the pressure distribution, shows that the pressure in the channels decreases with increasing distance along the process air flow channels. The distributions also indicates that the pressure will decrease equally for all channels. This is a reasonable distribution since all the flow channels are identical, the process air enters the channels at the same conditions and the temperature distribution indicates that the air properties will effectively remain constant.

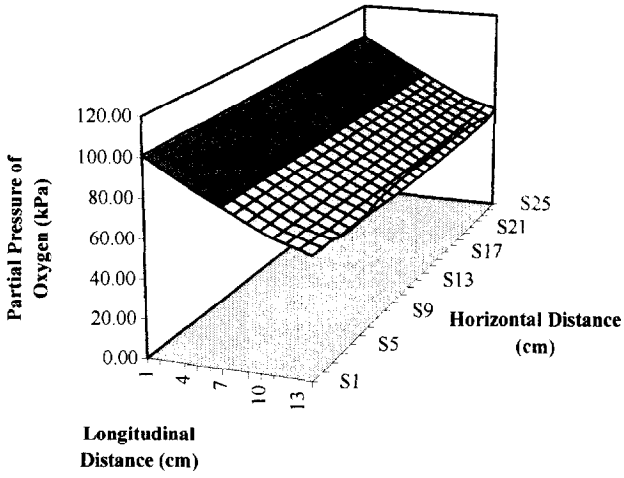

Fig. 10. Plot of the relative humidity distribution of the center MEA of a PEMFC stack after 15 min of simulation.

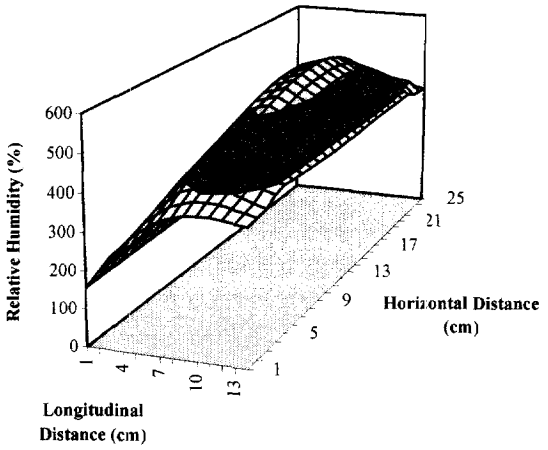

Fig. 11. Plot of the partial pressure of oxygen distribution of the center MEA of a PEMFC stack after 15 min of simulation.

The distribution of the relative humidity for the process air is shown in Fig. 10. Initially the relative humidity of the process air increases as it moves through the fuel cell (longitudinal distance). However, as the process air continues longitudinally through the fuel cell the relative humidity of the air begins to decrease. This results because the increased temperature of the process air increases it's capacity to hold water.

Liquid water forms in the cathode, as indicated by relative humidity greater than 100%, however the volume of water is not sufficient to completely block the process air flow channels located in the bipolar plate (see Fig. 2). The model of the fuel cell stack computes the amount of liquid water and checks to ensure that the air passages of the bipolar plate remain open.

The distribution of the partial pressure of oxygen is shown in Fig. 11. The partial pressure varies primarily in the longitudinal direction with a significant reduction in partial pressure with increasing longitudinal distance. The initial region of the MEA produces more current than the later regions, due to the greater oxygen concentration (see Eq. (5)), and therefore uses larger amounts of oxygen. As a result, the rate of decrease in the partial pressure of oxygen will reduce with increasing longitudinal distance. The slight variation in partial pressure with lateral position is a result of variations in MEA performance.

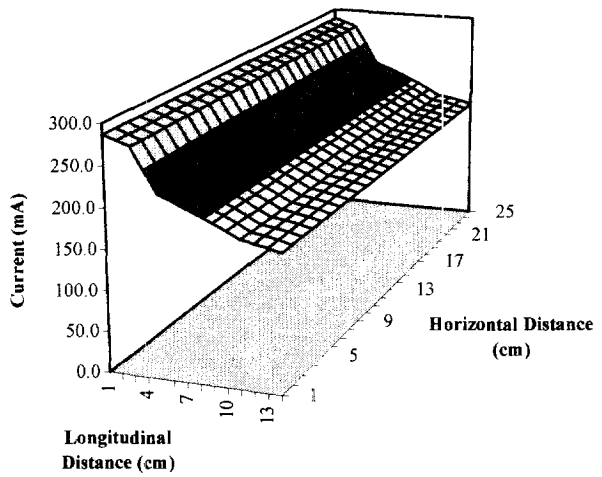

Fig. 12. Plot of the current distribution of the center MEA of a PEMFC stack after 15 min of simulation.

The current distribution, given in Fig. 12, shows a strong relationship between the partial pressure of oxygen and current production. The two curves are very similar in shape with the area of highest current production corresponding to the area of highest oxygen concentration. The current production is greatest as the product air enters the fuel cell stack, area of greatest oxygen concentration, and reduces with increasing lateral position. The current production does not vary significantly in the lateral direction further indicating that the oxygen concentration has the largest effect on current production.

5. Conclusions

A technique for numerically modeling the Membrane-Electrode Assemblies (MEA) of Proton Exchange Membrane Fuel Cell (PEMFC) stacks was developed. The MEA model is part of a numerical model of a complete fuel cell stack. The model uses a family of empirical equations that describe the electrochemical characteristics of a MEA in combination with methods for satisfying the electrical requirements of fuel cell stacks. The objective was to develop a model that would simulate the performance of the MEAs in large scale fuel cell stacks without extensive calculations.

The modeling technique was used to model the MEA of a PEMFC stack and output from the model was given and discussed. Results included plots of the temperature, pressure, humidity, oxygen partial pressure, and current distributions. It was determined that the MEA model developed using the technique and combined with a model of a complete fuel cell power system produced results that were reasonable when compared to established performance expectations and experimental results [12–14].

This modeling technique is a useful tool for investigating fuel cell power system MEAs. The model can be used to investigate the effect of local temperature, pressure, humidity, and oxygen concentration variations on MEA performance. In addition, the model can be used to investigate different MEA design and assembly methods by changing the coefficients of the polarization equations used to describe the electrochemical performance of the MEA. The coefficients would be determined from the results of laboratory scale single cell experiments.

Acknowledgements

The authors would like to thank the National Highway Institute, a division of the Department of Transportation,

and the Center for Electrochemical Systems and Hydrogen Research at Texas A&M University for sponsoring this work.

Appendix A. Derivation of voltage correction

Consider the case where the power is not correct but the current is. The correction would be to divide the power change equally between all the cells in the stack.

$$(\Delta V_{\mathrm{MEA}})_k = \frac{\Delta P_{\mathrm{Stack}}}{K i_{\mathrm{MEA}}} \tag{19}$$

Next, consider the case where the current is not correct but the power is. Since the power is correct it will be assumed to remain the same. Then:

$$V_{\mathrm{MEA}} i_{\mathrm{MEA}} = P_{\mathrm{MEA}} = (V_{\mathrm{MEA}} i_{\mathrm{MEA}})_{\mathrm{new}} \tag{20}$$

$$(V_{\mathrm{MEA}})_{\mathrm{new}} = \frac{P_{\mathrm{MEA}}}{(i_{\mathrm{MEA}})_{\mathrm{new}}} \tag{21}$$

Where the new MEA current is defined in Eq. (22):

$$(i_{\mathrm{MEA}})_{\mathrm{new}} = i_{\mathrm{MEA}} + \frac{(i_{\mathrm{MEA}})_{\mathrm{mean}} - i_{\mathrm{MEA}}}{K} = \frac{1}{K}\left((i_{\mathrm{MEA}})_{\mathrm{mean}} + (K-1) i_{\mathrm{MEA}}\right) \tag{22}$$

This is done so that the correction for each MEA is unique and therefore make the current from each MEA more equal. Substituting Eq. (22) for the new MEA current Eq. (21) becomes:

$$(V_{\mathrm{MEA}})_k = \frac{K(P_{\mathrm{MEA}})_k}{(i_{\mathrm{MEA}})_{\mathrm{mean}} + (K-1)(i_{\mathrm{MEA}})_k} \tag{23}$$

Combine Eqs. (19) and (23) to obtain the total voltage correction for a cell.

$$(V_{\mathrm{MEA}})_k = \frac{K(P_{\mathrm{MEA}})_k}{(i_{\mathrm{MEA}})_{\mathrm{mean}} + (K-1)(i_{\mathrm{MEA}})_k} + \frac{\Delta P_{\mathrm{Stack}}}{K i_{\mathrm{MEA}}} \tag{24}$$

References

[1] T.E. Springer, T.A. Zawodzinski, J. Electrochem. Soc. 138 (1991) 2334.
[2] A. Kihlidi, B. Lafage, P. Taxil, M.J. Clifton, Int. J. Hydrogen Energy 19 (1994) 245.
[3] T.V. Nguyen, R.E. White, J. Electrochem. Soc. 140 (1993) 2178.
[4] F. Kreith, M.S. Bohn, Principles of Heat Transfer, 4th edn., Harper & Row, New York, 1986, p. 595.
[5] A.J. Appleby, F.R. Foulkes, Fuel Cell Handbook, Van Nostrand-Reinhold, 1989, p. 22.
[6] L.J.M.J. Blomen, M.N. Mugerwa, Fuel Cell Systems, Plenum, New York, 1993, p. 110.
[7] S.W. Angrist, Direct Energy Conversion, 3rd edn., Allyn and Bacon, Boston, 1976, p. 380.
[8] A.J. Appleby, Comprehensive Treatise on Electrochemistry, Vol. 7, Plenum, New York, 1983, p. 173.
[9] J. Kim, S. Supramaniam, C.E. Chamberlin, J. Electrochem. Soc. 142 (1995) 2670.
[10] J.H. Lee, T.R. Lalk, Proc. ASME Winter Annual Meeting, Atlanta, GA, Nov. 1996.
[11] G.H. Cole, SAE Technical Paper Series, No. 891664, Society of Automotive Engineers, 1989.
[12] R.J. Lawrance, V.A. Margiott, SAE Technical Paper Series, No. 899174, Society of Automotive Engineers, 1989.
[13] Y.W. Rho, Y.T. Kho, S. Srinivasan, J. Electrochem. Soc. 141 (1994) 2084.
[14] R.D. Sutton, N.E. Vanderbourgh, Electrochemical Engine System Modeling and Development, Proc. U.S. DOE Annual Automotive Technology Development Contractors' Meeting, Nov. 1992.